J|A|C|S
ARTICLES
Published on Web 05/24/2006

Mechanistic Analysis of Reductive Nitrosylation on Water-Soluble Cobalt(III)-Porphyrins

Federico Roncaroli and Rudi van Eldik*

Contribution from the Institute for Inorganic Chemistry, University of Erlangen-Nürnberg, Egerlandstrasse 1, 91058 Erlangen, Germany

Received July 25, 2005; Revised Manuscript Received April 3, 2006; E-mail: vaneldik@chemie.uni-erlangen.de

Abstract: The reactions of NO and/or NO_2^- with three water-soluble cobalt porphyrins $[Co^{III}(P)(H_2O)_2]^n$, where P = TPPS, TCPP, and TMPyP, were studied in detail. At pH < 3, the reaction with NO proceeds through a single reaction step. From the kinetic data and activation parameters, the $[Co^{III}(P)(NO)(H_2O)]^n$ complex is proposed to be the primary product of the reaction with NO. This complex reacts further with a second NO molecule through an inner-sphere electron-transfer reaction to generate the final product, $[Co^{III}(P)(NO^-)]^{n-1}$. At pH > 3, although a single reaction step is also observed, a systematic study as a function of the NO and NO_2^- concentrations revealed that two reaction steps are operative. In the first, NO_2^- and NO compete to substitute coordinated water in $[Co^{III}(P)(H_2O)_2]^n$ to yield $[Co^{III}(P)(NO)(H_2O)]^n$ and $[Co^{III}(P)(NO_2^-)(H_2O)]^{n-1}$ as the primary reaction products. Only the nitrite complex could be detected and no final product formation was observed during the reaction. It is proposed that $[Co^{III}(P)(NO)(H_2O)]^n$ rapidly reacts with NO_2^- to form the nitrite complex, which in the second reaction step reacts with another NO molecule to generate the final product through an inner-sphere electron-transfer reaction. The reported results are relevant for the interaction of vitamin B_{12a} with NO and NO_2^-.

1. Introduction

Nitric oxide (NO) plays an important role in mammalian biochemistry in terms of intracellular signaling, immune response, vasodilatation, etc. Many of these processes involve reactions with metal centers.[1]

It has been proposed that vitamin B_{12} reacts with NO under physiological conditions which modifies the physiological action of NO.[2] In an earlier report from our laboratory, it was found that aquacobalamin (B_{12a}) does not react with NO at pH 7.[3a] The reason for this behavior was later studied using density functional and molecular orbital theoretical calculations.[3b] Nevertheless, it was reported later in the literature that B_{12a} can react with NO but only at low pH where the dissociation of the coordinated dimethylbenzimidazole group is favored through protonation.[4] The final product of the reaction was not a Co^{III}-(NO) complex but a Co^{II}(NO) complex (or formally $Co^{III}(NO^-)$), viz. the same product that is obtained in the reaction between reduced B_{12a} and NO,[5] from which it follows that reductive nitrosylation operates under these conditions. This finding may be of significant biological importance in order to understand the apparent inhibition of NO by vitamin B_{12a}. Co^{III}(P), P = porphyrin, complexes show a similar behavior, in which the reaction with NO results in Co^{II}(P)(NO) or $Co^{III}(P)(NO^-)$ as final product as shown in reaction 1.[6,7f]

$$Co^{III}(P) + 2NO \rightarrow\rightarrow Co^{III}(P)(NO^-) + NO_2^- \qquad (1)$$

The products were characterized by several techniques, viz. UV−vis,[6,7] IR,[7c−e,8] ^{15}N NMR,[5,8] and electrochemistry,[7] and the crystal structure was determined for some of them.[9] From IR spectroscopy, ν_{NO} was found to be close to 1700 cm^{-1}. From the crystal structure it was found that these complexes are pentacoordinate and the Co−N−O angle is close to 125°. This information indicates that the produced Co^{II}(NO) complexes are formally better described as $Co^{III}(NO^-)$ complexes.[5] In this

(1) (a) Palmer, R. M. J.; Ferrige, A. G.; Mocanda, S. *Nature* **1987**, *327*, 524. (b) Mocanda, S.; Palmer, R. M. J.; Higgs, E. A. *Pharmacol. Rev.* **1991**, *43*, 109−142. (c) Feelisch, M.; Stamler, J. S. Methods in Nitric Oxide Research, John Wiley and Sons: Chichester, England, 1996. (d) *Nitric Oxide: Biology and Pathobiology*; Ignarro, L. J., Ed.; Academic Press: San Diego, 2000.

(2) (a) Rochelle, L. G.; Morana, S. J.; Kruszyna, H.; Russell, M. A.; Wilcox, D. E.; Smith, R. P. *J. Pharmacol. Exp. Ther*. **1995**, *275*, 48. (b) Brouwer, M.; Chamulitrat, W.; Ferruzi, G.; Sauls, D. L.; Weinberg, J. B. *Blood* **1996**, *88*, 1857. (c) Greenberg, S. S.; Xie, J. M.; Kapusta, D. R.; Miller, M. J. S. *J. Pharmacol. Exp. Ther*. **1995**, *273*, 257. (d) Zheng, D.; Birke, R. *J. Am. Chem. Soc*. **2001**, *123*, 4637−4638. (e) Kruszyna, H.; Magyar, J. S.; Rochelle, L. G.; Russell, M. A.; Smith, R. P. *J. Pharmacol. Exp. Ther*. **1998**, *285*, 665.

(3) (a) Wolak, M.; Stochel, G.; Hamza, M.; van Eldik, R. *Inorg. Chem*. **2000**, *39*, 2018−2019. (b) Selcuki, C.; van Eldik, R.; Clark, T. *Inorg. Chem*. **2004**, *43*, 2828−2833.

(4) Sharma, V. S.; Pilz, R. B.; Boss, G. R.; Madge, D. *Biochemistry* **2003**, *42*, 8900−8908.

(5) Wolak, M. Zahl, A.; Schneppensieper, T.; Stochel, G.; van Eldik, R. *J. Am. Chem. Soc*. **2001**, *123*, 9780−9791.

(6) (a) Laverman, L. E.; Ford, P. C. *J. Am. Chem. Soc*. **2001**, *123*, 11614 − 11622. (b) Laverman, L. E. PhD Dissertation, University of California Santa Barbara, USA, 1999.

(7) (a) Fujita, E.; Fajer, J. *J. Am. Chem. Soc*. **1983**, *105*, 6743−6745. (b) Kelly, S.; Lancon, D.; Kadish K. M.; *Inorg. Chem*. **1984**, *23*, 1451−1458. (c) Fujita, E.; Chang, C. K.; Fajer, J. *J. Am. Chem. Soc*. **1985**, *107*, 7665−7669. (d) Kadish, K. M.; Mu, X. H.; Lin, X. Q. *Inorg. Chem*. **1988**, *27*, 1489−1492. (e) Mu, X. H.; Kadish, K. M. *Inorg. Chem*. **1990**, *29*, 1031−1036. (f) Cheng, S.; Su, Y. O. *Inorg. Chem*. **1994**, *33*, 5847−5854.

(8) Groombridge, C. J.; Larkworthy, L. F.; Mason, J. *Inorg. Chem*. **1993**, *32*, 379−380.

(9) (a) Ellison, M. K.; Scheidt, W. R. *Inorg. Chem*. **1998**, *37*, 382−383. (b) Scheidt, W. R.; Ellison, M. K. *Acc. Chem. Res*. **1999**, *32*, 350.

10.1021/ja0549906 CCC: $33.50

report, we will therefore refer to the final product of the reaction between NO and $Co^{III}(P)$ as $Co^{III}(P)(NO^-)$.

Some $Co^{III}(P)(NO)$ complexes have been characterized through UV−vis, IR, and EPR spectroscopy.[7] They were obtained through electrochemical oxidation of the corresponding $Co^{III}(P)(NO^-)$ complexes in organic solvents and were reported to be very unstable toward the dissociation of NO, i.e., NO is rapidly released with formation of $[Co^{III}(P)(solvent)_2]^n$ complexes.[7b]

The reductive nitrosylation of $Fe^{III}(P)$ complexes has been studied and is the subject of some reviews.[10] The reaction is catalyzed by NO_2^- and various bases. In the case of the Co analogues, reaction 1 is well-known to occur. As far as we know, there are no mechanistic or kinetic data available for this reaction.

This background information motivated us to explore the reactions of some water soluble $Co^{III}(P)$ complexes with NO. In this report, we present a detailed mechanistic study of these reactions, with special attention on the influence of NO_2^-, a common impurity in aqueous NO solutions, and pH. We obtained a completely different mechanistic picture than that reported for the corresponding iron porphyrin complexes before.

2. Experimental Section

2.1. Materials. NO 99.9% was purchased from Alpha Caz and purified from higher nitrogen oxides by passing through an Ascarite II (Aldrich) column. Co(III)-meso-tetra-(4-carboxyphenyl)-porphyrin was purchased from Porphyrin Systems, and Co(III)-meso-tetra-(4-sulfonatophenyl)-porphyrin acetate and Co(III)-meso-tetra-(4-methylpyridyl)-porphyrin tetratosylate acetate were purchased from Frontier Scientific. The purity of these complexes was checked by elemental analysis. $NaNO_2$ was obtained from Merck. The remaining chemicals were of analytical grade and used without further purification.

2.2. Methods. All solutions were prepared using distilled and purified water (Milli-Q system), deoxygenated upon N_2-saturation in Schlenk tubes and handled with gastight syringes. Acetate and MES (2-[N-morpholino]ethanesulfonic acid) (pH 4−6), citrate (pH 2−4), phosphate, bis-tris (bis[2-hydroxyethyl]imino-tris[hydroxymethyl]methane) (pH 6−8), and borate (pH 8−10) buffers were used at a concentration of 0.01 M to control the pH unless otherwise specified. $HClO_4$ solutions were used at pH lower than 2. The ionic strength was adjusted with $NaClO_4$ to 0.1 M. NO-saturated solutions were prepared by slowly bubbling NO through deoxygenated buffer solutions. The NO concentration of such solutions is already known from our earlier work on the subject, viz. 1.8×10^{-3} M at 25 °C.[11] The solutions were eventually diluted with buffer solutions to reach the desired NO concentration level. Complex solutions were prepared by dissolving the porphyrin complexes in the corresponding buffer or $HClO_4$ solutions. This procedure led to the formation of the diaqua complexes, viz. $[Co^{III}(TCPP)(H_2O)_2]^{3-}$, $[Co^{III}(TPPS)(H_2O)_2]^{3-}$ and $[Co^{III}(TMPyP)(H_2O)_2]^{5+}$ (TCPP = meso-tetra-(4-carboxyphenyl)-porphyrin, TPPS = meso-tetra-(4-sulfonatophenyl)-porphyrin, and TMPyP = meso-tetra-(4-*N*-methyl-pyridyl)-porphyrin).[12] pH measurements were done with a WTW inoLab level 1 pH meter at room temperature. EPR spectra were measured on the X-band of a Brucker ESP 300E spectrometer. The spectra were recorded at 140 K (frozen solution), 9.43 GHz, 0.635 mW power, 100 kHz modulation frequency, and 9.3434 G modulation amplitude.

2.3. Kinetic Experiments. Stopped-flow measurements were done on a SX-18 MV stopped-flow spectrophotometer from Applied Photophysics. The complex solutions ($2 \times 10^{-6} - 1 \times 10^{-5}$ M, 0.01 M in buffer, $I = 0.1$ M) were rapidly mixed with an equal volume of a NO and/or NO_2^- solution. Kinetic traces were monitored at 400 and 425 nm for $[Co^{III}(TPPS)(H_2O)_2]^{3-}$, 400 and 427 nm for $[Co^{III}(TCPP)(H_2O)_2]^{3-}$, and 413 and 433 nm for $[Co^{III}(TMPyP)(H_2O)_2]^{5+}$. They were fitted to single or double exponential functions depending on the observed kinetic trace using the SX-18 MV program. The traces obtained at pH < 3 were usually fitted to a single exponential. In those cases, where a two-exponential model was used, the amplitude of the second exponential was much smaller than that of the first. A single-exponential function was always enough to fit the kinetic traces for the formation of the product at 400−413 nm. On the other hand, the traces corresponding to the depletion of the Soret band of the starting complexes (425−433 nm) at pH > 3 in the presence of NO_2^-, were always fitted to a double exponential function. Most of the experiments were done in duplicate or in triplicate, the reported observed rate constants (k_{obs}) are the averages of 4−10 kinetic runs and the errors correspond to the standard deviation of the data.

To gain a clearer picture of the spectral changes, the most representative experiments were studied by rapid scan technique, which afforded complete spectral changes. These experiments were performed on the same stopped-flow instrument by connecting it to a J&M rapid scan detector, attached to a TIDAS 16−416 spectrophotometer. The spectra were analyzed by the SPECFIT program.[13] The slowest reactions ($k_{obs} < 1 \times 10^{-3}$ s^{-1}) were studied on a Varian Cary 5G spectrophotometer, equipped with a temperature control unit.

Most of the experiments were done at 25.0 ± 0.1 °C. For the NO_2^- concentration dependence, the final NO_2^- concentration ranged between 5×10^{-4} and 1.5×10^{-2} M, the buffer concentration was 0.025 M and the total ionic strength was 0.1 M. For the HNO_2 concentration dependence, the concentration was in the range $(1-5) \times 10^{-3}$ M, and solutions were 0.1 M in $HClO_4$. For the NO concentration dependence studies, the concentration was in the range $(2.3-9.0) \times 10^{-4}$ M, except for the $[Co^{III}(TMPyP)(H_2O)_2]^{5+}$ complex at pH 1.0 (0.1 M $HClO_4$), where the range was $(4.5-18) \times 10^{-4}$ M. For the experiments in which mixtures of NO and NO_2^- were used, $[NO] = (2.3-9.0) \times 10^{-4}$ M and $[NO_2^-] = (0-2) \times 10^{-3}$ M. Experiments at different HNO_2 concentrations ($1-5 \times 10^{-3}$ M) and NO (9.0×10^{-4} M) were done for the $[Co^{III}(TPPS)(H_2O)_2]^{3-}$ complex at 25.0 °C and pH = 1.0. For these experiments, a complex solution in 0.2 M $HClO_4$, was mixed in the stopped flow instrument with another solution, NO-saturated, with the necessary amount of $NaNO_2$, and without the addition of buffer or acid. This was done to avoid the loss of HNO_2 during saturation with NO. In a complementary experiment, a solution of 8.4×10^{-5} M $[Co^{III}(TCPP)(H_2O)_2]^{3-}$ was mixed with a NO-saturated solution of 2.24×10^{-3} M $NaNO_2$ (both solutions at pH 5.0, 0.01 M acetate buffer, $I = 0.1$ M $NaClO_4$, $T = 25.0$ °C). Kinetic traces were recorded at 543 nm and fitted with a two-exponential function.

(10) (a) Fernandez, B. O.; Lorkovic, I. M.; Ford, P. C.; *Inorg. Chem.* **2003**, *42*, 2−4. (b) Fernandez, B. O.; Lorkovic, I. M.; Ford, P. C.; *Inorg. Chem.* **2004**, *43*, 5393−5402. (c) Fernandez, B. O.; Ford, P. C.; *J. Am. Chem. Soc.* **2003**, *125*, 10510−10511. (d) Ford, P. C.; Fernandez, B. O.; Lim, M. D. *Chem. Rev.* **2005**, *105*, 2439−2456. (e) Goldstein, S.; Czapski, G. *J. Am. Chem. Soc.* **1995**, *117*, 12078−12084.

(11) (a) Roncaroli, F.; Olabe, J. A.; van Eldik, R. *Inorg. Chem.* **2003**, *42*, 4179−4189. (b) Roncaroli, F.; Olabe, J. A.; van Eldik, R. *Inorg. Chem.* **2002**, *41*, 5417−5425.

(12) (a) Abwao-Konya, J.; Cappelli, A.; Jacobs, L.; Krishnamurthy, M.; Smith, M. *Transition Met. Chem.* **1984**, *9*, 270−273. (b) Ashley, K. R.; Leipoldt, J. G. *Inorg. Chem.* **1981**, *20*, 2326−2333. (c) Ashley, K. R.; Au−Young, S. *Inorg. Chem.* **1976**, *15*, 1937−1939. (d) Pasternack, R. F.; Cobb, M. A.; Sutin, N. *Inorg. Chem.* **1975**, *14*, 866−873. (e) Pasternack, R. F.; Cobb, M. A. *J. Inorg. Nucl. Chem.* **1973**, *35*, 4327−4339. (f) Ashley R. K.; Berggren, M.; Cheng, M. *J. Am. Chem. Soc.* **1975**, *97*, 1422−1426. (g) Pasternack R. F.; Parr, G. R. *Inorg. Chem.* **1976**, *15*, 3087−3093. (h) Leipoldt, J. G.; van Eldik, R.; Kelm, H. *Inorg. Chem.* **1983**, *22*, 4146−4149.

(13) (a) Binstead, R. A.; Zuberbuhler, A. D. *SPECFIT*, Spectrum Software Associates, Chapel Hill, NC, 1993−1999. (b) Zuberbuhler, A. D. *Anal. Chem.* **1990**, *62*, 2220. (c) Origin 7, OriginLab Corporation, One Roundhouse Plaza, Northampton, MA 01060, USA. (d) *Experimental Physical Chemistry*; Bettelheim, F. A, W. B. Sanders Co.: Philadelphia, 1971. (e) *Handbook of Analytical Chemistry*; Meites, L, Ed.; MacGraw-Hill: New York, 1963.

Experiments at different temperatures (10−40 °C) were done for the $[Co^{III}(TPPS)(H_2O)_2]^{3-}$ complex in order to obtain the thermal activation parameters. The temperature was controlled with an accuracy of ± 0.1 °C with a Haake K20 thermostat. The reactions with NO at pH 1.0, with NO_2^- at pH 5.0 and with HNO_2 at pH 1.0 were studied at a single concentration (9.0×10^{-4} M, 1.0×10^{-2} M, and 5×10^{-3} M, respectively), neglecting any intercept in the plots of k_{obs} vs entering ligand concentration. All these experiments were done in duplicate. For the reaction with NO in the presence of NO_2^- at pH 5.0, 4.5×10^{-4} M and 9.0×10^{-4} M NO solutions, and 1×10^{-3} M NO_2^- were employed. The intercepts of the plots k_{obs} vs [NO] were calculated from the data for the reaction with NO_2^- at different temperatures. The second-order rate constants for these reactions were calculated and Eyring plots were constructed from which the thermal activation parameters were estimated. The same reactions were studied as a function of the pressure (100 − 1300 bar) with a custom-built high-pressure stopped-flow instrument described before.[14] The solutions employed and adopted procedures were similar to those described for the temperature dependence studies, except for the reaction with NO in the presence of NO_2^- where only 9.0×10^{-4} M NO solutions ($[NO_2^-] = 1 \times 10^{-3}$ M) were used.

The coordination of the second NO_2^- molecule to the $[Co^{III}(TPPS)(H_2O)_2]^{3-}$ complex was studied by preequilibrating solutions of the complex (8×10^{-6} M) and NO_2^- (8.3×10^{-4} M, pH = 5.0, I = 0.1 M) to form the 1:1 complex. After 2 h they were mixed in the stopped-flow with an equal volume of another NO_2^- solution ($[NO_2^-] = 2 \times 10^{-3} - 3 \times 10^{-2}$ M, pH = 5.0, 0.05 M acetate buffer, I = 0.1 M, T = 25.0 °C).

For preliminary experiments on the reaction between $[Co(TPPS)(NO^-)]^{4-}$ and HNO_2, a 7×10^{-6} M $[Co^{III}(TPPS)(H_2O)_2]^{3-}$ solution (in 0.2 M $HClO_4$) was saturated with NO and allowed to react for 1 h, after which it was mixed with a $NaNO_2$ solution ($1 \times 10^{-3} - 10 \times 10^{-3}$ M in water) in the stopped-flow instrument.

Linear plots were fitted with Microsoft Excel and the errors of the slopes and intercepts were calculated with the same program.

2.4. Thermodynamics of the Reaction with NO_2^-. To evaluate the equilibrium constant for the coordination of the first NO_2^- molecule to the $[Co^{III}(TPPS)(H_2O)_2]^{3-}$ complex (reaction 3), aliquots (10−250 μL) of the NO_2^- solution (8.17×10^{-4} M, pH = 5.0, 0.01 M acetate buffer, I = 0.1 M $NaClO_4$) were added to 5 mL of the complex solution (5.27×10^{-6} M, pH 5.0, 0.01 M acetate buffer, I = 0.1 M $NaClO_4$). The resulting solutions were allowed to react at 24.0 ± 0.5 °C for a period of 9 h, after which the spectra were recorded on the Cary 5G spectrophotometer. Using mass balances for the complex and NO_2^- concentration, the expression in (2) is obtained for the equilibrium constant (K_3) expressed in terms of concentration and absorbance.

$$K_3 = \frac{\dfrac{A - A_o}{A_\infty - A_o}}{\left(1 - \dfrac{A - A_o}{A_\infty - A_o}\right)\left([NO_2]_o - \dfrac{A - A_o}{A_\infty - A_o}[Co]_o\right)} \qquad (2)$$

In eq 2, A is the absorbance at the selected wavelength, A_o is the initial absorbance (in the absence of NO_2^-), A_∞ is the absorbance at a high NO_2^- concentration, $[NO_2^-]_o$ is the analytical concentration of nitrite, and $[Co]_o$ is the initial complex concentration. The absorbance values at 419, 425, 432, and 437 nm were fitted according to eq 3 using the program Origin 7.[13c] The values of K_3 and A_∞ were treated as variable parameters. Within the nitrite concentration range studied for the determination of K_3, the concentration of the bis-nitrite species is negligible according to the estimated value of K_4 from the kinetic data. The error in K_3 was estimated from the error of each fit and the different K_3 values at each wavelength. The errors in K_4 and k_{-3} were calculated propagating the errors of k_4 and k_{-4}, and k_3 and K_3, respectively, as described in the literature.[13d]

2.5. Titration of the $[Co(TPPS)(H_2O)_2]^{3-}$ Complex with NO. 9.00×10^{-5} M complex solutions were mixed with a certain volume of a NO-saturated solution (0.5−10 mL, final volume 20 mL, pH 5.0 in 0.05 M acetate buffer, I = 0.1 M $NaClO_4$). The solutions were allowed to react at 25 °C for 0.5−10 h depending on the NO concentration used. The solutions were then transferred to a 0.1 cm optical cell and the UV−vis spectra were recorded as described before. The spectra were corrected for the corresponding dilution factor.

2.6. Determination of the NO_2^-/HNO_2 Concentration. The concentration of NO_2^-/HNO_2 impurities in the NO solutions was determined by the UV−vis absorption of HNO_2 at low pH (0.1M $HClO_4$). HNO_2 shows a characteristic fingerprint spectrum with several maxima (molar absorbances determined from a calibration curve) at 386 nm ($\epsilon = 31.0 \pm 0.2$ M^{-1} cm^{-1}), 371 nm ($\epsilon = 51.8 \pm 0.5$ M^{-1} cm^{-1}), 358 nm ($\epsilon = 49.9 \pm 0.4$ M^{-1} cm^{-1}), 346 nm ($\epsilon = 36.6 \pm 0.3$ M^{-1} cm^{-1}), and 336 nm ($\epsilon = 23.7 \pm 0.1$ M^{-1} cm^{-1}). These data are in excellent agreement with data reported in the literature.[3a,10e] Although the molar absorbances are low, the characteristic fine structure makes it easy to observe this band at low concentrations and in the presence of other absorbing species. This is not the case for the NO_2^- species, which has a band at 354 nm ($\epsilon = 21$ M^{-1} cm^{-1})[10e] and does not show the fine structure. On the other hand, both species NO_2^- and HNO_2 show bands below 250 nm,[10e] which are highly unspecific since many other substances absorb in this region and are therefore not suitable for NO_2^-/HNO_2 analyses. This procedure was checked using the *Griess* reaction.[1c,13e] The latter technique was used to determine the concentration of NO_2^- generated during the reaction with NO at pH 5.0. For this purpose, a 9.00×10^{-5} M $[Co^{III}(TPPS)(H_2O)_2]^{3-}$ solution was saturated with NO and allowed to react for 15 min. After this time, 5 mL of the solution was mixed with an equal volume of a 1% sulfanilic acid (in 30% acetic acid) solution. After one minute the resulting solution was mixed with 5 mL of a 1% α-naphthylamine (in 30% acetic acid) solution. The final solution was allowed to react at room temperature for 15 min, after which the absorbance at 532 nm was determined. The same procedure was followed for a saturated NO solution. Two independent determinations were done for the Co complex and for the NO solution. The reported result is an average of these measurements. A calibration curve was constructed using the same procedure (concentration range $(5.8-49.0) \times 10^{-5}$ M NO_2^-, Abs (532 nm) = $1380[NO_2^-] + 0.020$, $R^2 = 0.9997$).

3. Results and Discussion

3.1. Reaction of $[Co(TPPS)(H_2O)_2]^{3-}$ with NO at pH 5. Figure 1 shows the spectral changes that correspond to the reaction of a 3.5×10^{-6} M solution of $[Co(TPPS)(H_2O)_2]^{3-}$ with 9.0×10^{-4} M NO (pH = 5.0, I = 0.1, T = 25.0 °C). The Soret band of the reactant (425 nm, $\epsilon = 2.5 \times 10^5$ M^{-1} cm^{-1}) decreases whereas a new band at 413 nm ($\epsilon = 1.2 \times 10^5$ M^{-1} cm^{-1}) assigned to the formation of $[Co(TPPS)(NO^-)]^{4-}$ appears.[6] Analogous spectral changes are observed in the Q-band (542 nm) although of much smaller intensity. Both the position of the bands and the molar absorptions are in agreement with data reported in the literature.[6,12b]

The final spectrum is also obtained when $[Co(TPPS)(H_2O)_2]^{3-}$ is first reduced with $Na_2S_2O_4$ or $NaBH_4$, and then allowed to react with NO. Kinetic traces at 425 and 400 nm show first-order behavior with an observed rate constant (k_{obs}) of 4.0×10^{-3} s^{-1}. Similar spectral changes and rate constants have been reported in the literature for the reaction of $Co^{III}(P)$ with NO.[6b] A careful investigation of the isosbestic points at 358, 420 and 447 nm, shows that it is not a very clean reaction. Moreover,

(14) van Eldik, R.; Gaede, W.; Wieland, S.; Kraft, J.; Spitzer, M.; Palmer, D. A. *Rev. Sci. Instrum.* **1993**, *64*, 1355. (b) van Eldik, R.; Palmer, D. A.; Schmidt, R.; Kelm, H. *Inorg. Chim. Acta* **1981**, *50*, 131.

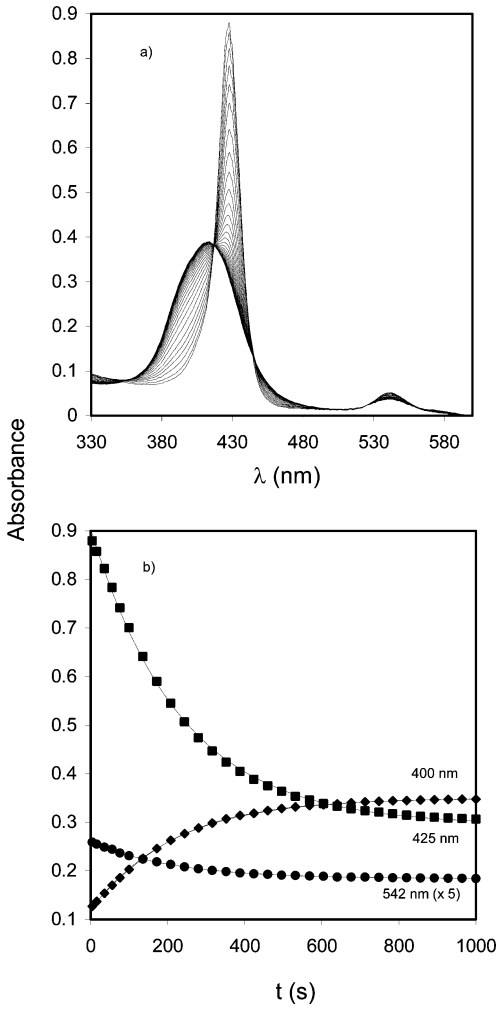

Figure 1. (a) UV−vis spectral changes observed during the reaction of the $[Co(TPPS)(H_2O)_2]^{3-}$ complex with NO. $[Co(TPPS)(H_2O)_2^{3-}] = 3.5 \times 10^{-6}$ M, $[NO] = 9.0 \times 10^{-4}$ M, pH = 5.0 (0.01 M acetate buffer), $I = 0.1$ M ($NaClO_4$), $T = 25.0$ °C. (b) Kinetic traces at 400, 425 and 542 nm (the last one was multiplied by 5 to fit the scale). $k_{obs} = 4.0 \times 10^{-3}$ s^{-1}.

in some cases, kinetic traces had to be fitted to a two-exponential function pointing toward a more complex kinetic behavior.

Solutions of this complex were titrated with NO (see Figure S1), from which we conclude that 2 equivalents of NO are consumed during this reaction, which is in very good agreement with the overall stoichiometry expressed by eq 1. Furthermore, the formation of NO_2^- during the reaction was determined (see Figure S2). For a 9.00×10^{-5} M complex solution, the NO_2^- concentration increased by 1.1×10^{-4} M as compared to the NO saturated solution. In other words, 1.2 mol of NO_2^- are produced per mole of complex. This is also in close agreement with the stoichiometry expressed by eq 1.

Several groups have reported that NO_2^- and/or HNO_2 are common impurities in aqueous NO solutions.[3a,10b] These come from higher nitrogen oxides present in the NO gas and/or from traces of O_2 present in the solutions that react with NO. The source of O_2 is not only due to inefficient de-oxygenation, but also due to traces of O_2 present or adsorbed in the instruments (viz. stopped-flow, cells, etc). It is known that O_2 and NO rapidly react in aqueous solution to produce NO_2^-, for which the third-order rate constant is 2.88×10^6 M^{-2} s^{-1}.[10e] We observed that NO_2^- impurities increase with time over several months. For this reason NO bottles were never stored for longer than 6 months. We concluded that the major source of NO_x came from the NO bottle itself. These NO_x (N_2O_3, NO_2, N_2O_4, etc.) compounds are unstable in water and rapidly generate NO_2^- under an excess of NO[10d,e] (N_2O is also an impurity but is virtually inert). Although the preparation of clean NO solutions in organic solvents has been claimed in the literature,[15] we were unable to reach NO_2^- concentration levels below 5×10^{-5} M in aqueous solution. Typical NO_2^- concentration levels in the present study were $(2 \pm 1) \times 10^{-4}$ M. For this reason, we first investigated the reaction between $[Co(TPPS)(H_2O)_2]^{3-}$ and NO_2^- (reaction 3), followed by a study of the reaction with mixtures of NO and NO_2^-.

3.2. Reaction of $[Co(TPPS)(H_2O)_2]^{3-}$ with NO_2^- at pH 5. During reaction 3 of the complex with NO_2^-, the Soret band of the starting complex decreases slightly and shifts from 425 to 427 nm ($\epsilon = 2.3 \times 10^5$ M^{-1} cm^{-1}).

$$[Co(TPPS)(H_2O)_2]^{3-} + NO_2^- \underset{k_{-3}}{\overset{k_3}{\rightleftharpoons}} [Co(TPPS)(NO_2)(H_2O)]^{4-} + H_2O \; K_3 \quad (3)$$

The equilibrium constant for this reaction (K_3) was found to be $(3.9 \pm 0.4) \times 10^5$ M^{-1} (pH = 5.0, $I = 0.1$ M, $T = 24.0$ °C) as calculated from the observed spectral changes (see Figure 2, Experimental Section, and in Figure S3 the optical difference spectra are shown).

The plot of k_{obs} vs $[NO_2^-]$ (included in Figure 5) showed a linear dependence with a zero intercept. The rate constant for this reaction (k_3) was found to be 38.5 ± 0.8 M^{-1} s^{-1} (pH = 5.0, $I = 0.1$ M, $T = 25.0$ °C). From the kinetic data (k_3) and the equilibrium constant (K_3), the value of k_{-3} was estimated to be $(1.0 \pm 0.1) \times 10^{-4}$ s^{-1}. The activation parameters were determined for the reaction with nitrite and found to be $\Delta H^{\ddagger} = 90.2 \pm 0.6$ kJ/mol, $\Delta S^{\ddagger} = +88 \pm 2$ J/Kmol and $\Delta V^{\ddagger} = +11 \pm 1$ cm^3/mol (see plots included in Figures 8 and 9). Similar activation parameters were obtained for substitution reactions with other ligands such as pyridine, SCN^-, and I^- (see Table 1), for which a dissociative mechanism was proposed.[12b,h]

The 1:1 nitrite complex can react further with NO_2^- to produce a 1:2 nitrite complex as shown in reaction 4.

$$[Co(TPPS)(H_2O)(NO_2^-)]^{4-} + NO_2^- \underset{k_{-4}}{\overset{k_4}{\rightleftharpoons}} [Co(TPPS)(NO_2)_2]^{5-} + H_2O \; K_4 \quad (4)$$

The values of k_4 and k_{-4} were found to be $(3.4 \pm 0.6) \times 10^3$ M^{-1} s^{-1} and 28.7 ± 0.8 s^{-1}, respectively, from which a value of 120 ± 20 M^{-1} was estimated for K_4. Evidently, the coordination of a second NO_2^- is significantly faster than the first one. This behavior was observed for this type of complex with several ligands and was explained in terms of the *trans*-labilization effect or the increase in electron density on the Co(III) center after ligand coordination, which gives the metal center some Co(II) character.[12a,b]

3.3. Reaction of $[Co(TPPS)(H_2O)_2]^{3-}$ with NO_2^- and NO at pH 5. Figure 3a shows the spectral changes observed during the reaction of $[Co(TPPS)(H_2O)_2]^{3-}$ with a mixture of NO_2^-

(15) Lim, M. D.; Lorkovic, I. M.; Wedeking, K.; Zanella, A. W.; Works, C. F.; Massick, S. M.; Ford, P. C. *J. Am. Chem. Soc.* **2002**, *124*, 9737−9743.

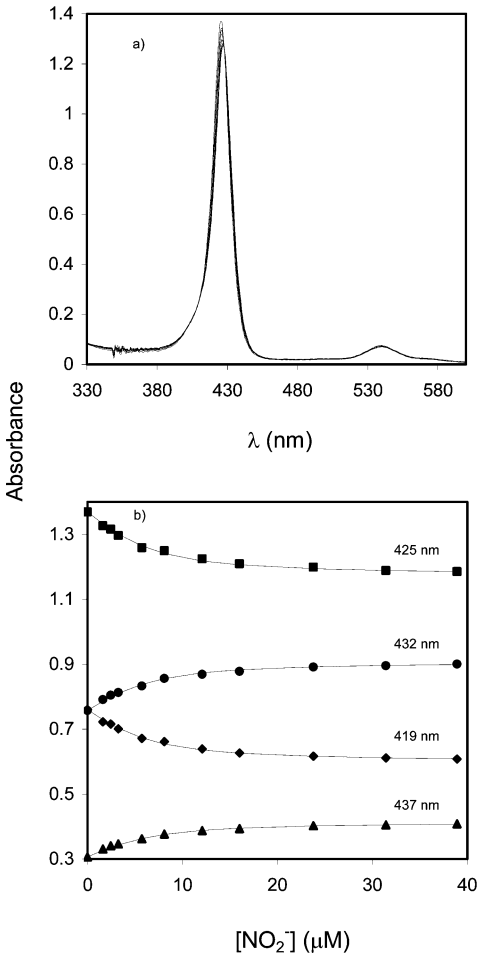

Figure 2. (a) UV−vis spectra of the $[Co(TPPS)(H_2O)_2]^{3-}$ complex in the presence of different concentrations of NO_2^-. $[Co(TPPS)(H_2O)_2^{3-}] = 5.27 \times 10^{-6}$ M, pH = 5.0 (0.01 M acetate buffer), $I = 0.1$ M ($NaClO_4$), $T = 24.0$ °C. (b) Absorbance at selected wavelengths fitted to eq 2. $K_3 = (3.9 \pm 0.4) \times 10^5$ M^{-1}. (See Experimental Section for analysis of data).

and NO ($[NO_2^-] = 1.03 \times 10^{-3}$ M, $[NO] = 9.0 \times 10^{-4}$ M, pH = 5.0, $T = 25.0$ °C, $I = 0.1$ M). Figure 3b shows the kinetic traces at the most relevant wavelengths. Two reaction steps are clearly observed; the observed rate constant for the first reaction ($k_{1(obs)}$) is 6.5×10^{-2} s^{-1} and for the second reaction step ($k_{2(obs)}$) is 3.9×10^{-3} s^{-1}. The spectral changes were analyzed by SPECFIT[13] and three species were detected. In Figure 3c, the spectra corresponding to the reactant, intermediate and product species are shown. The product has the same UV−vis spectral properties as the one obtained in the reaction without the addition of NO_2^-. The intermediate shows a maximum at 427 nm that closely resembles the product of the reaction with only NO_2^-. It is worth noting that during the first reaction step practically no formation of the final product is observed.

We performed a systematic study of both reaction steps by varying the NO concentration and keeping the NO_2^- concentration constant, and vice versa. Figure 4 shows the observed rate constants for the first and second reaction steps ($k_{1(obs)}$ and $k_{2(obs)}$, respectively) as a function of the NO concentration in the presence of 8.64×10^{-4} M NO_2^-. Both data sets show linear concentration dependences. The slope for the first reaction (k_1) equals 37 ± 5 M^{-1} s^{-1} with an intercept of $(3.4 \pm 0.3) \times 10^{-2}$ s^{-1}. The second reaction does not show a significant intercept with a slope (k_2) of 4.5 ± 0.5 M^{-1} s^{-1}. The intercept of the

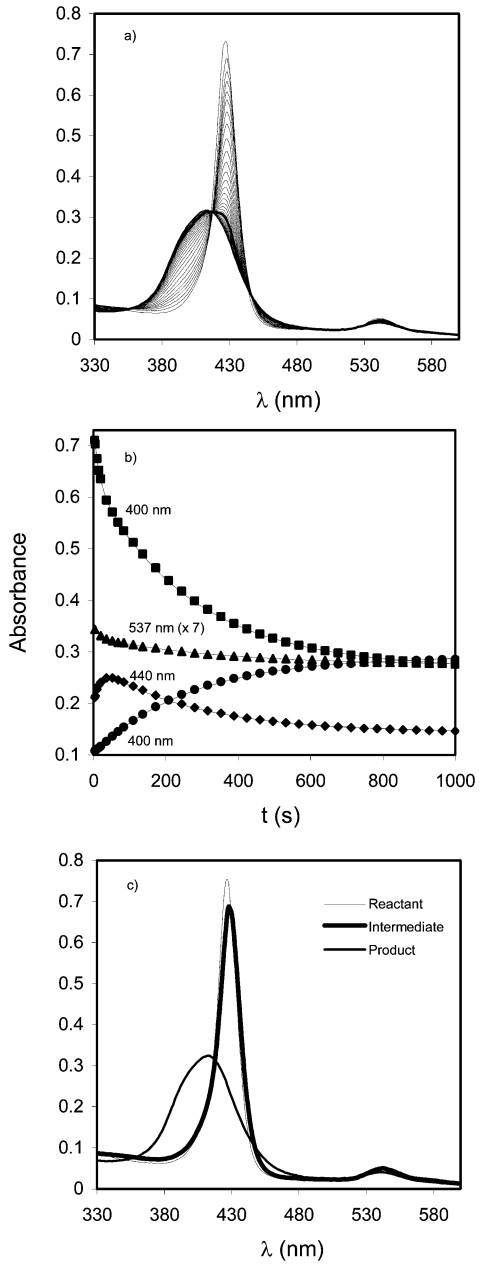

Figure 3. (a) UV−vis spectral changes observed during the reaction of the $[Co(TPPS)(H_2O)_2]^{3-}$ complex with NO in the presence of NO_2^-. $[Co(TPPS)(H_2O)_2^{3-}] = 2.9 \times 10^{-6}$ M, $[NO_2^-] = 1.03$ mM, pH = 5.0 (0.01 M acetate buffer), $I = 0.1$ M ($NaClO_4$), $T = 25.0$ °C. (b) Kinetic traces at 537, 440, 425, and 400 nm analyzed using a two-exponential model, $k_{1(obs)} = 6.5 \times 10^{-2}$ s^{-1}, $k_{2(obs)} = 3.9 \times 10^{-3}$ s^{-1} (the trace at 537 nm was multiplied by 7 to fit the scale). (c) Spectra of the reactant, intermediate, and product obtained from spectral analysis with SPECFIT.

plot of $k_{1(obs)}$ vs [NO] is in agreement with that expected for the reaction of $[Co(TPPS)(H_2O)_2]^{3-}$ with NO_2^- under the selected conditions, i.e., $(3.33 \pm 0.07) \times 10^{-2}$ s^{-1}. The $k_{2(obs)}$ values are very similar to the k_{obs} values obtained in the absence of added NO_2^-, where only one reaction step was in principle observed. We can mention here that k_1 is close to the value of the slope of the plot of k_{obs} vs [NO], k_6, obtained at pH 1.0, viz. 32 ± 1 M^{-1} s^{-1}, under which conditions very little or no appreciable second reaction step is observed. Furthermore, the error introduced by the HNO_2 impurities is much smaller, since HNO_2 reacts with a lower rate constant, viz. $k_7 = 14.2 \pm 0.4$ M^{-1} s^{-1} (vide infra).

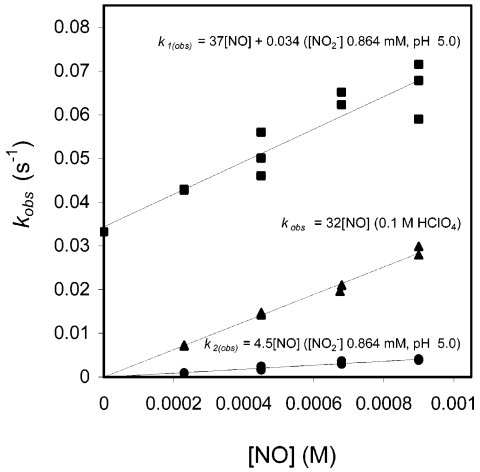

Figure 4. NO concentration dependence for the reaction with $[Co(TPPS)(H_2O)_2]^{3-}$ studied under different conditions. pH = 5.0 (0.01 M acetate buffer) or pH = 1.0 ($HClO_4$), I = 0.1 M ($NaClO_4$), T = 25.0 °C, $[Co(TPPS)(H_2O)_2^{3-}] = 1-5 \times 10^{-6}$ M. Different values of k_{obs} represent the spread in the measurements at a particular NO concentration (each data point is the average of 4 to 10 kinetic runs).

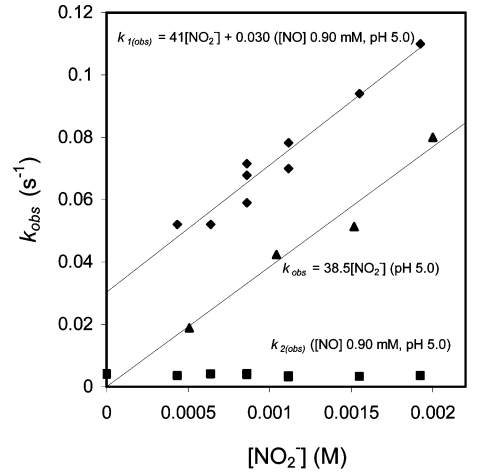

Figure 5. NO_2^- concentration dependence of the observed rate constant for the first and second reaction steps with $[Co(TPPS)(H_2O)_2]^{3-}$ in the presence of NO. Some data that correspond to the NO_2^- concentration dependence in the absence of NO are also shown ($[NO_2^-] = 5.1 \times 10^{-4} - 1.49 \times 10^{-2}$ M). pH = 5.0 (0.01 M acetate buffer), I = 0.1 M ($NaClO_4$), T = 25.0 °C, $[Co(TPPS)(H_2O)_2^{3-}] = 1-5 \times 10^{-6}$ M. Different values of k_{obs} represent the spread in the measurements at a particular NO_2^- concentration (each data point is the average of 4 to 10 kinetic runs).

Analogously, we performed experiments keeping the NO concentration constant at 9.0×10^{-4} M and changing systematically the NO_2^- concentration. In this case we also observed two reaction steps as before. Plots of $k_{1(obs)}$ and $k_{2(obs)}$ vs $[NO_2^-]$ are shown in Figure 5 (some data corresponding to the reaction with NO_2^- in the absence of NO are also shown for comparison purposes). The data corresponding to the first reaction ($k_{1(obs)}$) again show a linear concentration dependence. The slope of the line, viz. 41 ± 4 M^{-1} s^{-1} is in close agreement with the second-order rate constant for the coordination of the first NO_2^- molecule to the Co(III) complex, viz. 38.5 ± 0.8 M^{-1} s^{-1}. Furthermore, the intercept of this plot, viz. $(3.0 \pm 0.4) \times 10^{-2}$ s^{-1}, is in agreement with the k_{obs} value of the reaction with NO (9.0×10^{-4} M) in the absence of NO_2^-, viz. $(2.9 \pm 0.1) \times 10^{-2}$ s^{-1}. It is important to note that as the NO_2^- concentration decreases, the absorbance change corresponding to the first reaction step also decreases. This may offer an explanation for why the first reaction step was not observed when no NO_2^- was added. The $k_{2(obs)}$ values did not show a significant NO_2^- concentration dependence under the selected conditions, at least in the range $4.3 \times 10^{-4} - 1.92 \times 10^{-3}$ M. We did not study

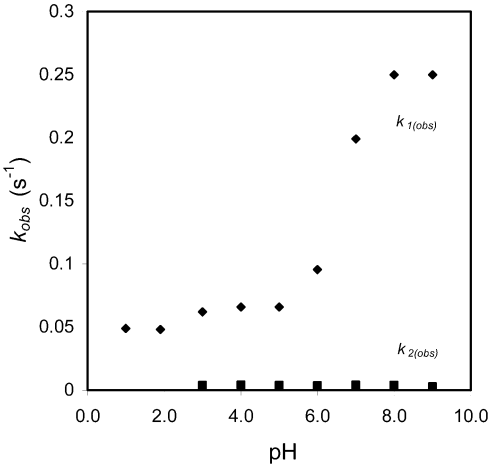

Figure 6. pH dependence of the observed rate constants for the first and second reaction steps of the $[Co(TPPS)(H_2O)_2]^{3-}$ complex. [NO] = 9.0×10^{-4} M, $[NO_2^-] = (0.86-1.16) \times 10^{-3}$ M, I = 0.1 M ($NaClO_4$), T = 25.0 °C, [buffer] = 0.01 M, $[Co(TPPS)(H_2O)_2^{3-}] = 1-5 \times 10^{-6}$ M.

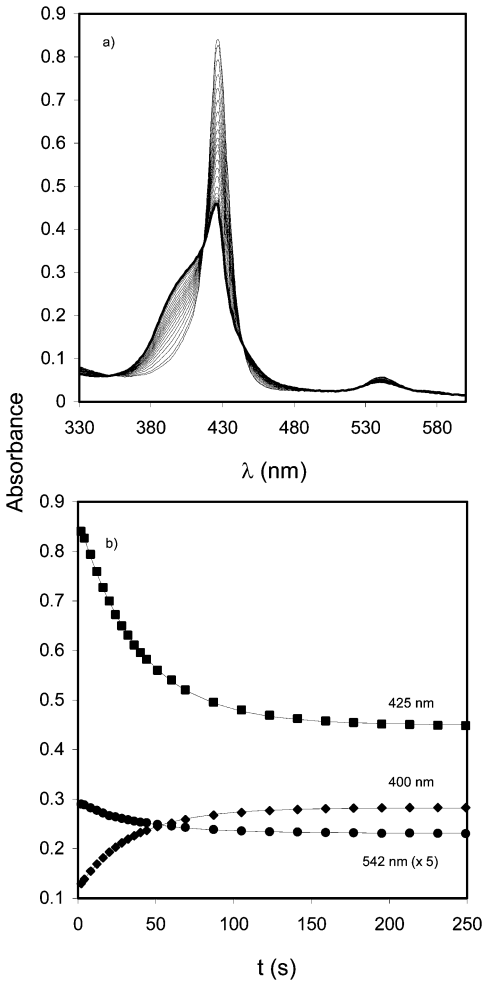

Figure 7. (a) UV−Vis spectral changes observed during the reaction of $[Co(TPPS)(H_2O)_2]^{3-}$ with NO. $[Co(TPPS)(H_2O)_2^{3-}] = 3.3 \times 10^{-6}$ M, [NO] = 9.0×10^{-4} M, 0.1 M $HClO_4$, T = 25.0 °C. (b) Kinetic traces at 542, 425 and 400 nm, $k_{obs} = 2.7 \times 10^{-2}$ s^{-1} (traces at 542 nm had to be multiplied by 5 to fit the scale).

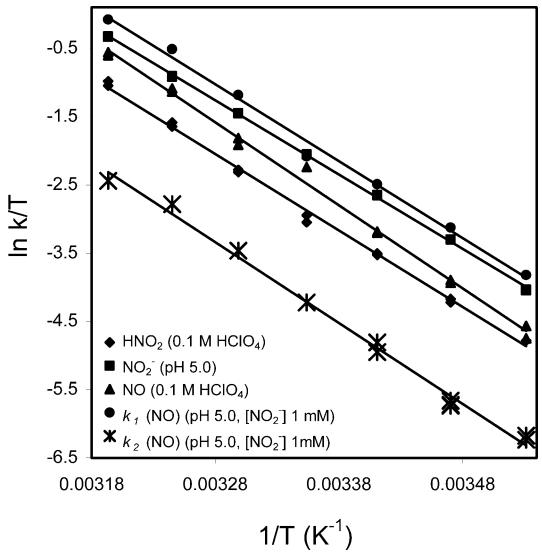

Figure 8. Eyring plots for the different reactions studied for the $[Co(TPPS)(H_2O)_2]^{3-}$ complex. $T = 10-40$ °C, $I = 0.1$ M ($NaClO_4$). See Table 1 for the thermal activation parameters. See Experimental Section for the selected conditions.

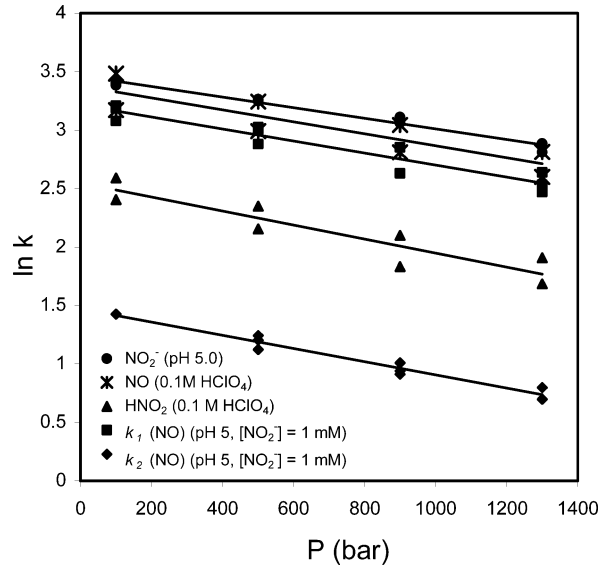

Figure 9. Pressure dependence of the different reactions studied for the $[Co(TPPS)(H_2O)_2]^{3-}$ complex. P = 100−1300 bar, $T = 25.0$ °C, $I = 0.1$ M ($NaClO_4$). See Table 1 for the activation volumes. See Experimental Section for the selected conditions.

the reaction for NO_2^- concentrations higher than 2×10^{-3} M in detail, since under such conditions the kinetic traces are more complex, probably due to the coordination of the second NO_2^- molecule to the Co(III) complex. Despite this, experiments at 2.6×10^{-3} and 5.0×10^{-3} M NO_2^- showed $k_{2(obs)}$ values of $(3.5 \pm 0.3) \times 10^{-3}$ s^{-1} (measured at 400 nm).

All this experimental evidence clearly shows that in the first reaction, NO and NO_2^- compete for the Co(III) center, and the observed rate constant can be written as in eq 5. We do not have any evidence for a catalytic effect of NO_2^- as was the case for the $Fe^{III}(P)$ complexes.[10]

$$k_{1(obs)} = k_6[NO] + k_3[NO_2^-] \quad (5)$$

In eq 5, k_6 corresponds to the second-order rate constant for the reaction of $[Co(TPPS)(H_2O)_2]^{3-}$ with NO generating the $[Co(TPPS)(H_2O)(NO)]^{3-}$ complex according to reaction 6. The reasons for this proposal are discussed in the section devoted to the mechanism of the reaction.

$$[Co(TPPS)(H_2O)_2]^n + NO \underset{k_{-6}}{\overset{k_6}{\rightleftharpoons}} [Co(TPPS)(NO)(H_2O)]^n + H_2O \; K_6 \quad (6)$$

For the second reaction step, the experimental data are consistent with a reaction of NO with $[Co(TPPS)(NO_2)(H_2O)]^{4-}$. EPR measurements performed during the reaction at pH 5.0 showed only silent spectra. As mentioned before, the UV−vis spectrum of the intermediate is very similar to the one obtained through direct reaction with NO_2^-. The NO_2^- concentration dependence for the first reaction step clearly shows that $[Co(TPPS)(NO_2)(H_2O)]^{4-}$ is formed. Finally, a solution of the diaqua complex preequilibrated with NO_2^- to generate the $[Co(TPPS)(NO_2)(H_2O)]^{4-}$ complex, reacts with NO at the same rate constants described above, viz. $(3.9 \pm 0.7) \times 10^{-3}$ s^{-1} at $[NO] = 9.0 \times 10^{-4}$ M.

We determined the activation parameters for both the reactions by working at different NO concentrations ($[NO_2^-]$ ca. 10^{-3} M), temperature and pressure (see Table 1 and plots in Figures 8 and 9): $\Delta H_1^{\ddagger} = 94 \pm 3$ kJ/mol, $\Delta S_1^{\ddagger} = +100 \pm 10$ J/Kmol and $\Delta V_1^{\ddagger} = +13 \pm 1$ cm^3/mol, $\Delta H_2^{\ddagger} = 98 \pm 3$ kJ/mol, $\Delta S_2^{\ddagger} = +97 \pm 9$ J/Kmol and $\Delta V_2^{\ddagger} = +14 \pm 1$ cm^3/mol. The data are clearly consistent with a dissociative substitution mechanism as found for the reaction with NO_2^- and other ligands.[12b,h]

Some experiments were also performed at different pH values ($[NO_2^-] = (0.86-1.16) \times 10^{-3}$ M, $[NO] = 9.0 \times 10^{-4}$ M, $I = 0.1$ M, $T = 25.0$ °C, see Figure 6). At pH lower than 3, where HNO_2 is the predominant nitrite species in solution, the second reaction is practically not observed and $k_{1(obs)}$ is around 5×10^{-2} s^{-1} (these data will be discussed later). At pH 3−5, where NO_2^- predominates, two reactions were clearly seen with $k_{1(obs)}$ ca. 6×10^{-2} s^{-1} and $k_{2(obs)}$ ca. 4×10^{-3} s^{-1} in agreement with our earlier results. At pH 6−8, an increase in $k_{1(obs)}$ was observed (viz. 2.5×10^{-1} s^{-1} at pH = 8.0), consistent with the deprotonation of one of the coordinated water molecules in the Co(III) complex, generating the $[Co(TPPS)(H_2O)(OH)]^{4-}$ species. The pK_a for this equilibrium is reported to be 7.0.[12b] In previous reports on ligand substitution reaction of this complex with pyridine and SCN^-, an increase in the reactivity was also found under such conditions.[12b] This was ascribed to the translabilization effect of coordinated OH^-. Interestingly, the $k_{2(obs)}$ values do not change appreciably in the pH range 3−8. These data, together with the activation parameters, show again that the first reaction step is controlled by the substitution of water in the $[Co(TPPS)(H_2O)_2]^{3-}$ complex.

Most of the experiments were performed using acetate buffer, whereas others were done with MES buffer, but no appreciable difference was observed. In some cases the complex solutions were prepared at pH = 3.0 ($HClO_4$) without the addition of $NaClO_4$, and the NO_2^-/NO solutions were prepared using a double concentrated buffer and ionic strength (pH = 5.0, $I = 0.2$ M). No appreciable difference was observed, indicating that neither the buffer nor ClO_4^- coordinates to the metal center under these conditions. An experiment in which the complex concentration was 4.2×10^{-5} M, showed no appreciable

Table 1. Kinetic Data for Reactions of NO and NO_2^- with the $[Co(TPPS)(H_2O)_2]^{3-}$ Complex[a]

reaction	k_1, $M^{-1}\,s^{-1}$ [intercept, s^{-1}]	k_2, $M^{-1}\,s^{-1}$ [intercept, s^{-1}]	$\Delta H^{\ddagger}_1$, kJ/mol	$\Delta H^{\ddagger}_2$, kJ/mol	$\Delta S^{\ddagger}_1$, J/Kmol	$\Delta S^{\ddagger}_2$, J/Kmol	$\Delta V^{\ddagger}_1$, cm^3/mol	$\Delta V^{\ddagger}_2$, cm^3/mol
NO (pH 1.0)	32 ± 1		101 ± 2		$+121 \pm 6$		$+13 \pm 1$	
NO_2^- (pH 5.0)	38.5 ± 0.8		90.2 ± 0.6		$+88 \pm 2$		$+11 \pm 1$	
HNO_2 (pH 1.0)	14.2 ± 0.4 $[(7 \pm 1) \times 10^{-3}]$		93 ± 2		$+91 \pm 5$		$+15 \pm 1$	
NO ($[NO_2^-]$ 1 mM, pH 5.0)	37 ± 5 $[(3.4 \pm 0.4) \times 10^{-2}]$	4.5 ± 0.5	94 ± 3	98 ± 3	$+100 \pm 10$	$+97 \pm 9$	$+13 \pm 1$	$+14 \pm 1$
NO_2^- ([NO] 0.9 mM, pH 5.0)	41 ± 4 $[(3.0 \pm 0.4) \times 10^{-2}]$	$[(4.2-3.2) \times 10^{-3}]$						
HNO_2 ([NO] 0.9 mM, pH 1.0)	13 ± 1 $[(3.4 \pm 0.5) \times 10^{-2}]$							
SCN^-	179[b]		77[c]		+60[c]		+15.4[d]	
Py	520[b]		74[c]		+60[c]			
I^-	118[c]		87[c]		+87[c]			

[a] $I = 0.1$ M, unless otherwise stated; subscripts 1 and 2 refer to the first and second observed reaction steps. [b] From ref 12a. [c] From ref 12b, $I = 1.0$ M. [d] From ref 12h, $I = 1.0$ M.

differences with the results reported above, viz. $k_{1(obs)} = (7.1 \pm 0.4)$ x 10^{-2} s^{-1} and $k_{2(obs)} = (3.3 \pm 0.5) \times 10^{-3}$ s^{-1} ($[NO_2^-] = 1.12 \times 10^{-3}$ M, [NO] $= 9.0 \times 10^{-4}$ M, pH 5.0, $T = 25.0$ °C), from which we conclude that the complex concentration does not affect the kinetics. Finally, an experiment at $I = 1.0$ M (pH 5.0, $[NO_2^-] = 8.3 \times 10^{-4}$ M, [NO] $= 9.0 \times 10^{-4}$ M) was done. $k_{1(obs)}$ increased to 0.14 ± 0.01 s^{-1}, which is consistent with the coordination of NO_2^- to a negatively charged complex, whereas $k_{2(obs)}$ did not change significantly, viz. $(3.9 \pm 0.1) \times 10^{-3}$ s^{-1}. In this experiment, kinetic traces at 425 nm showed some other complications which are probably related to the coordination of a second NO_2^- molecule, which is favored by the increase in ionic strength.

3.4. Reaction of $[Co(TPPS)(H_2O)_2]^{3-}$ with HNO_2 and NO at pH 1. The reaction with HNO_2 was studied at pH $= 1.0$ (0.1 M $HClO_4$) in the absence of NO. A plot of k_{obs} vs $[HNO_2]$ (see Figure S4, Supporting Information) showed a linear dependence with an appreciable intercept. The slope and the intercept can be related to k_7 and k_{-7}, respectively, according to reaction 7.

$$[Co(TPPS)(H_2O)_2]^{3-} + HNO_2 \underset{k_{-7}}{\overset{k_7}{\rightleftharpoons}} [Co(TPPS)(NO_2)(H_2O)]^{4-} + H_3O^+ \; K_7 \quad (7)$$

The obtained values for k_7 and k_{-7}, are 14.2 ± 0.4 $M^{-1}\,s^{-1}$ and $(7 \pm 1) \times 10^{-3}$ s^{-1}, respectively. The fact that k_{-7} and k_{-3} are quite different indicates that presumably H^+ catalysis is involved in the dissociation (back) reaction. The activation parameters for the complex-formation (forward) reaction are: $\Delta H^{\ddagger} = 93 \pm 2$ kJ/mol, $\Delta S^{\ddagger} = +91 \pm 5$ J/Kmol and $\Delta V^{\ddagger} = +15 \pm 1$ cm^3/mol (see plots included in Figures 8 and 9).

Figure 7 reports the spectral changes recorded during the reaction of $[Co(TPPS)(H_2O)_2]^{3-}$ with NO (9.0×10^{-4} M) at pH $= 1.0$ (0.1 M $HClO_4$). A first-order process is observed, but not all of the reactant is converted into the product. To acquire a 100% conversion, saturation with NO is required. We believe that the lower yield is due to impurities of HNO_2, or HNO_2 produced during the reaction (vide supra), that can oxidize the final product back to the reactant or to the nitro complex. In fact, preliminary stopped-flow experiments showed that HNO_2 reacts with the $[Co(TPPS)(NO^-)]^{4-}$ complex (i.e., $k_{obs} = 0.94 \pm 0.07$ s^{-1} for [NO] $= 9.0 \times 10^{-4}$ M, $[HNO_2] = 1.08 \times 10^{-3}$ M, pH 1.0). Nevertheless, we do not have any evidence that this reaction affects the kinetics of the reaction of $[Co(TPPS)(H_2O)_2]^{3-}$ with NO.

The kinetic traces were usually fitted to a single-exponential function. In cases where a two-exponential function was required, the amplitude of the second one was very small. In Figure 4, a plot of k_{obs} vs [NO] at pH 1.0 is also included. The data show a linear concentration dependence and no significant intercept, with a slope, k_6, of 32 ± 1 $M^{-1}\,s^{-1}$. As mentioned before, the value of the slope is in agreement with the data obtained in the presence of NO_2^- at pH 5.0. The activation parameters determined at pH 1.0 were found to be $\Delta H^{\ddagger} = 101 \pm 2$ kJ/mol, $\Delta S^{\ddagger} = +121 \pm 6$ J/Kmol and $\Delta V^{\ddagger} = +13 \pm 1$ cm^3/mol (see plots included in Figures 8 and 9), which are again consistent with a dissociative substitution mechanism. During the reaction an intermediate was detected, which showed a very weak EPR signal (see Figure S5). The assignment of this spectrum will be discussed later.

We performed some experiments at pH 1.0, keeping the NO concentration constant (9.0×10^{-4} M) and varying systematically the HNO_2 concentration (see Figure S4). A similar picture to the one previously reported for pH 5.0 was observed. The data show a linear concentration dependence with a slope 13 ± 1 $M^{-1}\,s^{-1}$, which is close to the slope obtained in the absence of NO (k_7), viz. 14.2 ± 0.4 $M^{-1}\,s^{-1}$. The intercept is $(3.4 \pm 0.5) \times 10^{-2}$ s^{-1}, which can be considered as the sum of k_{-7} ($(7 \pm 1) \times 10^{-3}$ s^{-1}) and k_6[NO] ($(2.9 \pm 0.1) \times 10^{-2}$ s^{-1}) under the selected conditions. Again, HNO_2 competes with NO to coordinate to the $[Co(TPPS)(H_2O)_2]^{3-}$ complex as for NO_2^-, although less effectively due to protonation, and eq 5 is still applicable. It is worth noting that formation of the final product, [Co(P)(NO^-)], is observed from the beginning of the reaction, in contrast to that observed at pH 5, where no conversion into this product was observed in the first reaction step. Finally, Figures 8 and 9 show the Eyring plots, and plots of ln k vs P for the studied temperature and pressure dependences. The kinetic data are summarized in Table 1 along with earlier published data on related substitution reactions.[12]

3.5. Reactions of $[Co(TCPP)(H_2O)_2]^{3-}$ and $[Co(TMPyP)(H_2O)_2]^{5+}$ with NO_2^- and NO. Since the $[Co(TCPP)(H_2O)_2]^{3-}$ complex is not soluble in water at pH lower than 5, the reactions were studied at pH 6.0, i.e., far enough from the pK_a value of the coordinated water, which was reported to be close to 7.5.[12g] The complex reacts with NO_2^- under pseudo-first-order conditions with a second-order rate constant, k_3, of 54.1 ± 0.2 $M^{-1}\,s^{-1}$ at 25.0 °C. Again, the back reaction was negligible and a zero intercept was observed in the plot of k_{obs} vs $[NO_2^-]$. The

Table 2. Kinetic Data for the Different Co(III) Porphyrin Complexes Studied[a]

	$[Co(TPPS)(H_2O)_2]^{3-}$		$[Co(TCPP)(H_2O)_2]^{3-}$		$[Co(TMPyP)(H_2O)_2]^{5+}$	
reaction	k_1, M^{-1} s^{-1} [intercept, s^{-1}]	k_2, M^{-1} s^{-1} [intercept, s^{-1}]	k_1, M^{-1} s^{-1} [intercept, s^{-1}]	k_2, M^{-1} s^{-1} [intercept, s^{-1}]	k_1, M^{-1} s^{-1} [intercept, s^{-1}]	k_2, M^{-1} s^{-1} [intercept, s^{-1}]
NO (pH 1.0)	32 ± 1				$(1.5 \pm 0.1) \times 10^{-1}$	
NO_2^- (pH[b])	38.5 ± 0.8		54.1 ± 0.2		8.4 ± 0.2	
HNO_2 (pH 1.0)	14.2 ± 0.4 $[(7 \pm 1) \times 10^{-3}]$					
NO ($[NO_2^-]$ 1 mM, pH[b])	37 ± 5 $[(3.4 \pm 0.3] \times 10^{-2}]$	4.5 ± 0.5	130 ± 10 $[(5.3 \pm 0.1) \times 10^{-2}]$	7.2 ± 0.5	1.6 ± 0.2 $[(8.4 \pm 0.1) \times 10^{-3}]$	2.2 ± 0.3
NO_2^- ([NO] 0.9 mM, pH[b])	41 ± 4 $[(3.0 \pm 0.4) \times 10^{-2}]$	$[(3.2-4.2) \times 10^{-3}]$	47 ± 6 $[(1.2 \pm 0.1) \times 10^{-1}]$	$[(5.3-6.7) \times 10^{-3}]$	8.8 ± 0.8	$[(1.6-2.4) \times 10^{-3}]$
SCN^-	179[c]		450[e]		2.1[f]	
Py	520[c]		1400[e]		0.7[f]	
I^-	118[d]				1.6[g]	
pK_a	7.0[d]		7.5[e]		6.0[f]	

[a] $T = 25.0$ °C, $I = 0.1$ M, unless otherwise stated; subscripts 1 and 2 refer to the first and second observed reaction steps. [b] pH = 5.0 for TPPS complex, pH = 6.0 for TCPP complex, and pH = 4.7 for TMPyP complex. [c] From ref 12a. [d] From ref 12b, $I = 1.0$ M. [e] From ref 12g, $I = 0.5$ M. [f] From ref 12d, $I = 0.5$ M. [g] From ref 12f, $I = 1.0$ M.

reaction with NO ($[NO] = 9.0 \times 10^{-4}$ M, without the addition of NO_2^-) proceeds through a single reaction step with a rate constant of $(6.4 \pm 0.8) \times 10^{-3}$ s^{-1} and with spectral changes similar to those described for the $[Co(TPPS)(H_2O)_2]^{3-}$ complex. Some experiments were done in the presence of NO_2^- (1.00×10^{-3} M), and varying the NO concentration (see Figure S6). Two reactions were observed as for the earlier studied complex. Plots of $k_{1(obs)}$ and $k_{2(obs)}$ vs [NO] showed linear concentration dependences. For the first reaction the slope was found to be 130 ± 10 M^{-1} s^{-1} and the intercept $(5.3 \pm 0.1) \times 10^{-2}$ s^{-1} (see Figure S6). The latter value is in agreement with the data for the coordination of NO_2^-. The plot for the second reaction showed a zero intercept and a slope of 7.2 ± 0.5 M^{-1} s^{-1}. In addition, experiments at a constant NO concentration (9.0×10^{-4} M) were also done (see Figure S7). The data corresponding to the first reaction had a slope of 47 ± 6 M^{-1} s^{-1} and an intercept of $(1.2 \pm 0.1) \times 10^{-1}$ s^{-1}, which are in agreement with the previous data for the coordination of NO_2^- and NO, respectively. This information is summarized in Table 2. A similar picture to the one already described for the $[Co(TPPS)(H_2O)_2]^{3-}$ complex is observed, in which both NO_2^- and NO compete in the first reaction, as described by eq 5. The second reaction was independent of the NO_2^- concentration in the range $(0.43-2.09) \times 10^{-3}$ M. Both of the reactions for the $[Co(TCPP)(H_2O)_2]^{3-}$ complex are faster than for the $[Co(TPPS)(H_2O)_2]^{3-}$ complex, consistent with the higher electron density on the metal center, as previously found for substitution with pyridine and SCN^- (see Table 2).[12a,b]

The reaction of $[Co(TMPyP)(H_2O)_2]^{5+}$ with NO_2^- behaves similar to the other two complexes described above. The plot of k_{obs} vs $[NO_2^-]$ again showed a linear concentration dependence with a zero intercept, for which the slope was found to be 8.4 ± 0.2 M^{-1} s^{-1} at 25.0 °C. The reaction with NO at pH = 1.0 is much slower than for the other studied complexes, viz. $(1.5 \pm 0.1) \times 10^{-1}$ M^{-1} s^{-1} (see Figure S8). Reactions with NO were also studied in the presence of NO_2^- at pH = 4.7, and two reaction steps were observed as expected. For the experiments at constant NO_2^- concentration (1.03×10^{-3} M) and variable NO concentration, the plot of $k_{1(obs)}$ vs [NO] shows an intercept of $(8.4 \pm 0.1) \times 10^{-3}$ s^{-1} (see Figure S8), which is in agreement with the kinetic data for the coordination of NO_2^- to this complex. The slope of 1.6 ± 0.2 M^{-1} s^{-1} is much larger than the second-order rate constant found at pH 1.0 for the reaction with NO. We believe that this slope is due to NO_2^- impurities in the NO solution, which are typically $(2 \pm 1) \times 10^{-4}$ M for a saturated NO solution. $k_{2(obs)}$ also depends linearly on the NO concentration. The plot of $k_{2(obs)}$ vs [NO] has a slope of 2.2 ± 0.3 M^{-1} s^{-1} and no significant intercept. Experiments at a constant NO concentration (9.0×10^{-4} M), were also done (see Figure S9). The plot of $k_{1(obs)}$ vs $[NO_2^-]$ has a slope of 8.8 ± 0.8 M^{-1} s^{-1}, in agreement with the data for the coordination of NO_2^-, and without a significant intercept, which is in agreement with the low second-order rate constant for the coordination of NO (viz. $(1.5 \pm 0.1) \times 10^{-1}$ M^{-1} s^{-1}, pH = 1.0). $k_{2(obs)}$ did not depend significantly on the $[NO_2^-]$ as found for the other two complexes and has a value of ca. 1.7×10^{-3} s^{-1} (see Figure S6).

For the $[Co(TMPyP)(H_2O)_2]^{5+}$ complex, although eq 5 is still valid, NO cannot compete with NO_2^- at pH 4.7. In general, all the reactions were slower for this complex than for the others, in agreement with earlier reports (see Table 2), which can be related to the electron density on the metal center.[12a,b] It is interesting to note that for the $[Co(TCPP)(H_2O)_2]^{3-}$ complex, k_6 is larger than k_3; for the $[Co(TPPS)(H_2O)_2]^{3-}$ complex these rate constants are very similar, and for the $[Co(TMPyP)(H_2O)_2]^{5+}$ complex, k_3 is larger than k_6. This finding may also be related to the total charge on the complex and particularly the charge on the metal center. From this it is reasonable to conclude that the positively charged complex will have a higher affinity for NO_2^- than for NO.

From a comparison of the values of k_6 and k_2, it follows that for $[Co(TPPS)(H_2O)_2]^{3-}$ and $[Co(TCPP)(H_2O)_2]^{3-}$ k_6 is larger than k_2, but for $[Co(TMPyP)(H_2O)_2]^{5+}$ the situation is the opposite (see Table 2). In fact, for the latter complex we could think in terms of NO_2^- catalysis, since NO_2^- coordinates in a first reaction step (NO cannot compete with this reaction) and then the intermediate, $[Co(TMPyP)(NO_2)(H_2O)]^{4+}$, reacts further with NO faster than the diaqua complex. The NO_2^- ligand reduces the positive charge on the metal center and makes it more reactive. Moreover, the reaction at pH 4.7 in the absence of external NO_2^- proceeds through a single reaction step with $k_{obs} = (1.2 \pm 0.1) \times 10^{-3}$ s^{-1} ($[NO] = 9.0 \times 10^{-4}$ M, 25 °C), for which we believe that the reaction with NO_2^- impurities controls the rate of the reaction.

3.6. Proposed Mechanism. 3.6.1. Reaction with NO at Low pH. The $[Co(TPPS)(H_2O)_2]^{3-}$ and $[Co(TMPyP)(H_2O)_2]^{5+}$ com-

plexes react with NO at pH 1 and show a linear NO concentration dependence without a significant intercept. The activation parameters are similar to those obtained for other entering nucleophiles and consistent with the dissociative substitution of coordinated water.[12b,h] Nevertheless, the final products are [Co(P)(NO^-)] complexes, indicating that a reductive nitrosylation process is operative. On the basis of our kinetic data, we propose that the reaction is controlled by the reversible substitution of coordinated water by NO to produce the [Co(P)(NO)(H_2O)] complex, eq 6. Such complexes have been obtained through electrochemical oxidation of the corresponding [Co(P)(NO^-)] complexes.[7] In all cases, they were obtained in organic, noncoordinating solvents, and were very unstable toward NO dissociation in the presence of ligands, i.e., NO is rapidly released with formation of $[Co^{III}(P)(solvent)_2]^n$ complexes.[7b] For this reason, we assume that K_6 must be very small in water. These complexes were characterized by IR, UV−vis and EPR spectroscopy.[7] In fact, the EPR spectrum of a solution of $[Co(TPPS)(H_2O)_2]^{3-}$ saturated with NO at pH = 1.0 ($HClO_4$) shows a weak signal that could be assigned to this intermediate (see Figure S5).[7c] The intermediate described in eq 6 reacts further in the presence of an excess of NO to produce the final product, [Co(P)(NO^-)]. This subsequent reaction is faster than the first one, such that no direct mechanistic information on this step could be obtained.

One possibility is that the [Co(P)(NO)(H_2O)] complex dissociates to generate NO^+ and a $[Co^{II}(P)(H_2O)]$ complex, which subsequently reacts rapidly under diffusion controlled conditions with another NO molecule to produce the final product (see eqs 8−9).[6] The problem with this mechanism is that NO^+ and HNO_2 oxidize $[Co^{II}(P)(H_2O)]$ complexes very effectively.

$$[Co^{III}(P)(NO)(H_2O)]^n \underset{k_{-8}}{\overset{k_8}{\rightleftharpoons}} [Co^{II}(P)(H_2O)]^{n-1} + NO^+ \; K_8 \quad (8)$$

$$[Co^{II}(P)(H_2O)]^{n-1} + NO \underset{k_{-9}}{\overset{k_9}{\rightleftharpoons}} [Co^{III}(P)(NO^-)]^{n-1} + H_2O \; K_9 \quad (9)$$

Such reactions have been proposed for the reductive nitrosylation of Fe(III) porphyrins, where base catalysis was observed (viz. nitrite, buffer, etc).[10] In the systems under study, there is no evidence in favor of such reactions, since the reductive nitrosylation of the water soluble cobalt porphyrins is observed even at pH 1.0, where NO_2^- that could be present is protonated and cannot act as an efficient nucleophile. Moreover, if base catalysis was operative, a stronger pH dependence should be observed, which could not be accounted for in terms of the pK_a of HNO_2 and the coordinated water molecule on the Co complex.

An alternative mechanism would involve the formation of a dinitrosyl complex, eq 10. This species would generate the final product through an inner-sphere electron-transfer step, eq 11.

$$[Co(P)(NO)(H_2O)]^n + NO \underset{k_{-10}}{\overset{k_{10}}{\rightleftharpoons}} [Co(P)(NO)_2]^n + H_2O \; K_{10} \quad (10)$$

$$[Co(P)(NO)_2]^n \xrightarrow{k_{11}} [Co(P)(NO^-)]^{n-1} + NO^+ \quad (11)$$

Formation of complexes of the type $[Co(P)(L)_2]$ was observed in all the earlier studies on ligand substitution reactions of [Co(P)(H_2O)$_2$] complexes (L = SCN, py, I^-).[12] Furthermore, we also observed this behavior for the reaction with NO_2^-. In all cases, coordination of the second nucleophile molecule was faster than the first, due to the increase in electron density on the metal center and/or trans-labilization effects. For these reasons, it is reasonable that a second NO molecule could coordinate and generate a dinitrosyl complex. Reaction 10 would also be faster than reaction 6 due to the strong trans-labilization effect of the NO ligand, which was observed for many other NO complexes. From another point of view, the electronic structure of the $[Co^{III}(P)(NO)(H_2O)]^n$ complex should include some contribution from the $[Co^{II}(P)(NO^+)(H_2O)]^n$ structure, and since $[Co^{II}(P)(L)]$ complexes tend to be pentacoordinate and square pyramidal, this provides a further reason for the lability of the coordinated water molecule trans to NO.

3.6.2 Reaction at Higher pH (4−9). Interference of NO_2^-. First Reaction Step, Competition between NO and NO_2^-. At pH 4−9, two reaction steps are observed when the [Co(P)(H_2O)$_2$] complexes react with mixtures of NO and NO_2^-. When no NO_2^- is added, the first reaction step is practically not detectable, probably due to the small spectral changes involved. As mentioned before, the first reaction can be described as a competition between NO and NO_2^-, and the observed rate constants ($k_{1(obs)}$) can be expressed by eq 5. The primary products of this reaction should be [Co(P)(NO)(H_2O)] and [Co(P)(NO_2)(H_2O)]. The puzzling observation was that practically *no formation of the final product* was observed during this reaction and only formation of [Co(P)(NO_2)(H_2O)] was observed. This observation led us to conclude that the intermediate [Co(P)(NO)(H_2O)] must be very unstable under these conditions, even more than at pH = 1.0. EPR measurements performed during the reaction of $[Co(TPPS)(H_2O)_2]^{3-}$ with NO at pH 5.0 always showed EPR silent spectra. We therefore propose that the [Co(P)(NO)(H_2O)] complex reacts rapidly with NO_2^- to produce the [Co(P)(NO_2)(NO)] complex, reaction 12, which eventually releases NO to produce the [Co(P)(NO_2)(H_2O)] complex, reaction 13. These type of complexes have been observed in Fe(II) porphyrin systems, where NO was also found to be labile.[15]

$$[Co(P)(NO)(H_2O)]^n + NO_2^- \underset{k_{-12}}{\overset{k_{12}}{\rightleftharpoons}} [Co(P)(NO_2)(NO)]^{n-1} + H_2O \; K_{12} \quad (12)$$

$$[Co(P)(NO_2)(NO)]^{n-1} + H_2O \underset{k_{-13}}{\overset{k_{13}}{\rightleftharpoons}} [Co(P)(NO_2)(H_2O)]^{n-1} + NO \; K_{13} \quad (13)$$

It is important to note that reaction 12 must be faster than reaction 10 under these pH conditions. We need to propose the intermediacy of the [Co(P)(NO_2)(NO)] complex in order to account for the formation of [Co(P)(NO_2)(H_2O)] while NO and NO_2^- indeed compete as nucleophiles. Reaction 12 is prevented at low pH due to protonation and formation of HNO_2, where formation of the [Co(P)(NO^-)] complex is *indeed* observed from the beginning of the reaction, even with the addition of small amounts of NO_2^-.

3.7. Second Reaction Step, Formation of the Final Product. This reaction shows a linear concentration dependence on

the NO concentration and no appreciable intercept for all the complexes studied. Furthermore, the reaction is independent of the NO_2^- concentration and the activation parameters are consistent with a dissociative mechanism.

This reaction, however, cannot be controlled by the dissociation of NO_2^-, because if this was the case it should show a strong NO_2^- concentration dependence. Moreover, according to the values obtained for k_3 and K_3 for $[Co(TPPS)(H_2O)_2]^{3-}$, k_{-3} is $(1.0 \pm 0.1) \times 10^{-4}$ s^{-1} and typical $k_{2(obs)}$ values are in the range $(1-4) \times 10^{-3}$ s^{-1}. Thus, it follows that the dissociation of NO_2^- cannot control the rate of the second step.

We also considered the possibility that the $[Co(P)(NO_2)(H_2O)]$ complex generates the final product by reacting with NO through the $[Co(P)(NO)_2]$ intermediate (reactions 10, 12, and 13). In this case, NO would induce the release of NO_2^-. Such a mechanism will only be in agreement with the kinetic data if $k_{10}[NO]$ is larger than $k_{12}[NO_2^-]$, which contradicts our earlier conclusion.

Oxo-transfer reactions have been extensively studied for many $Co^{III}(NO_2)$ systems, and particularly for porphyrin complexes.[16] In this type of reaction, an O-atom is transferred from the nitro complex to an acceptor such as alcohols, different saturated organic compounds, etc, whereby the complex is reduced to $Co^{III}(NO^-)$. The most classic O-acceptor is probably triphenylphosphine, which is very selective in these reactions. Recently, an oxo-transfer was proposed to be operative in the reaction between NO and sublimed layers of $Co(TPP)NO_2$, generating NO_2 and Co(TPP)NO (TPP = meso-tetraphenylporphyrin).[17] In principle, we would expect activation parameters consistent with an associative mechanism for such reactions. We performed some preliminary experiments on the reaction between $[Co(TCPP)(H_2O)_2]^{3-}$ and triphenylphosphine in the presence of NO_2^- in ethanol. We observed the formation of a new band at 415 nm which could be assigned to the final product, but the reactions were very slow (k_{obs} ca. 5×10^{-5} s^{-1} at 25 °C) and the dependence on the phosphine concentration was not linear, probably due to the coordination and competition with NO_2^-, which complicated the interpretation of the data. In conclusion, we do not have any evidence in favor of an oxo-transfer process in aqueous solution. Moreover, in these reactions the pentacoordinate nitro complex was found to be much more reactive than the hexa-coordinate complex,[16a,b] and the first one is not likely to be formed in aqueous solution where the hexacoodinate complex is strongly favored.

Finally, we propose that $[Co(P)(NO_2)(NO)]$, which is in equilibrium with $[Co(P)(NO_2)(H_2O)]$ (reaction 14), although at a very low concentration, can generate the same products as the oxo-transfer process through an inner-sphere electron-transfer reaction 15.

$$[Co(P)(NO_2)(H_2O)]^{n-1} + NO \underset{k_{-14}}{\overset{k_{14}}{\rightleftharpoons}} [Co(P)(NO_2)(NO)]^{n-1} + H_2O \; K_{14} \quad (14)$$

$$[Co(P)(NO_2)(NO)]^{n-1} \xrightarrow{k_{15}} [Co(P)(NO^-)]^{n-1} + NO_2 \quad (15)$$

Reaction 15 will be the rate-determining step for the second reaction step. The released NO_2 rapidly reacts with NO to form N_2O_3 ($k = 1.1 \times 10^9$ M^{-1} s^{-1}), which reacts with water to produce $2HNO_2$ ($k = 530$ s^{-1}).[10d,e] These reactions are much faster than the studied reactions, such that the NO_2 released in reaction 15 is rapidly converted to nitrite as final product. The expression for the observed rate constant of the second reaction step is given by eq 16 under the selected experimental conditions.

Scheme 1. Proposed Overall Mechanism for the Reductive Nitrosylation of Water-Soluble Co(III) Porphyrin Complexes

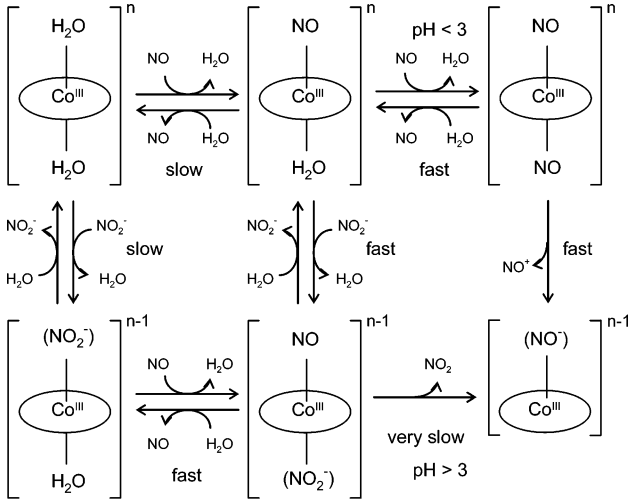

$$k_{2(obs)} = K_{14} \, k_{15} \, [NO] \quad (16)$$

This mechanism is consistent with the reported activation parameters, as well as with the NO and NO_2^- concentration dependences. The remarkably positive activation volume and entropy are consistent with a dissociative mechanism. The activation volume can be expressed, as in eq 17, as the sum of the contributions from reactions 14 and 15. An analogous expression can be derived for the activation entropy.

$$\Delta V^{\#} = \Delta V_{14} + \Delta V_{15}{}^{\#} \quad (17)$$

Reaction 14 involves the substitution of H_2O by NO, without spin or charge change and large entropy or volume changes are not expected. On the other hand, in reaction 15 there is an electronic reorganization and the release of the neutral molecule, NO_2, generating a pentacoordinate species, $[Co(P)(NO^-)]$. According to this, an increase in entropy and volume should occur during the reaction.

A correlation between the structure of the complexes and the rate of this reaction, k_2, is not straightforward, since complexes with a higher electron density and a higher lability (viz., the TCPP complex) should have a higher value of K_{14}, whereas more inert complexes but probably better oxidants (viz., the TMPyP complex) should have a higher value of k_{15}. Scheme 1 summarizes the overall proposed mechanism for the studied reactions based on all the arguments presented above.

(16) (a) Goodwin, J.; Kurtikyan, T.; Standard, J.; Walsh, R.; Zheng, B.; Parmley, D.; Howard, J.; Green, S.; Mardyukov, A.; Przybyla, D. E. *Inorg. Chem.* **2005**, *44*, 2215−2223. (b) Goodwin, J.; Bailey, R.; Pennington, W.; Rasberry, R.; Green, T.; Shasho, S.; Yongsavanh, M.; Echevarria, V.; Tiedecken, J.; Brown, C.; Fromm, G.; Lyerly, S.; Watson, N.; Long, A.; De Nitto, N. *Inorg. Chem.* **2001**, *40*, 4217−4225. (c) Tovrog, B. S.; Diamond, S. E.; Mares, F.; Szalkiewicz, A. *J. Am. Chem. Soc.* **1981**, *103*, 3522−3526. (d) Tovrog, B. S.; Mares, F.; Diamond, S. E. *J. Am. Chem. Soc.* **1980**, *102*, 6618 − 6619. (e) Tovrog, B. S.; Diamond, S. E.; Mares, F. *J. Am. Chem. Soc.* **1979**, *101*, 270−272.

(17) Kurtikyan, T. S.; Mardyukov, A. N.; Goodwin, J. A. *Inorg. Chem.* **2003**, *42*, 8489−8493.

Conclusions

The reactions of three different water-soluble Co(III) porphyrin complexes with NO were studied in detail. We confirmed that a reductive nitrosylation process is operative in all cases. We observed that two equivalents of NO are consumed during the reaction, which is in agreement with the stoichiometry proposed in eq 1 and strongly supports the proposed mechanism. Moreover, approximately one equivalent of NO_2^- is generated per mole of complex. The proposed mechanism differs largely from that previously suggested for reductive nitrosylation of Fe(III) porphyrins.[10] For these complexes, the product of the primary interaction with NO, $[Fe^{III}(P)(NO)(H_2O)]$, reacts with NO_2^-, bases or even with solvent to generate the $[Fe^{II}(P)]$ complex, which reacts further under diffusion controlled conditions with NO to produce the final product, $[Fe^{II}(P)NO]$.

We do not have evidence in favor of any kind of base catalysis as reported for the Fe(III) porphyrins.[10] We believe that the instability of the $[Co(P)(NO)(H_2O)]$ intermediate is responsible for this. Even if the electronic structure of this intermediate may have some contribution of the $[Co^{II}(P)(NO^+)(H_2O)]$ structure, its rapid decomposition in water prevents any reaction with other nucleophiles. In fact, such reactions are relatively slow for Fe complexes.[10] For example, the pseudo-first-order rate constant for the reaction of metHb(NO) with H_2O was determined to be 1.1×10^{-3} s^{-1}. The formation of Cyt^{II} from $Cyt^{III}-NO$ at a NO pressure of 100 Torr, has an observed rate constant that ranges from 1×10^{-3} to 5×10^{-3} s^{-1} when $[OH^-] = (1-4) \times 10^{-6}$ M. The reduction of $[Fe^{III}(TPPS)(H_2O)]^{3-}$ in the presence of NO (1.9×10^{-3} M) and acetic buffer (0.02−0.1 M) is characterized by rate constants between $(2-4) \times 10^{-4}$ s^{-1}, and the observed rate constant for the reductive nitrosylation of $[Fe^{III}(TMPyP)(H_2O)]^{5+}$ in the presence of NO_2^- ($5 \times 10^{-3} - 2.5 \times 10^{-2}$ M) ranges from 0.2 to 0.8 s^{-1}. Most of these reactions are even slower than the observed rate constants for the reactions between NO and Co porphyrins, viz. $(2.9 \pm 0.1) \times 10^{-2}$ s^{-1} for the reaction of $[Co(TPPS)(H_2O)_2]^{3-}$ with NO (9.0×10^{-4} M) at pH 1.0.

In our systems, at first sight the overall reaction seemed to proceed through a single reaction step, but a careful analysis in the presence of NO_2^- revealed that two reaction steps are involved. In the first reaction, NO and NO_2^- compete for coordination in $[Co(P)(H_2O)_2]$ (eq 5), which is supported by all the reported kinetic data and activation parameters. Moreover, in these reactions, NO and NO_2^- behave in the same way as other nucleophiles previously studied for these complexes. The $[Co(P)(NO)(H_2O)]$ complex is proposed to be the product of the primary interaction between NO and the diaqua complex (eq 6). This complex decomposes rapidly in the presence of NO_2^- to generate the $[Co(P)(NO_2)(H_2O)]$ complex (eqs 12 and 13), which is also the product of the reaction between NO_2^- and the starting compound. This reaction is prevented at low pH (due to protonation of nitrite), where only one reaction step is observed. Finally, we propose that the $[Co(P)(NO_2)(H_2O)]$ complex reacts with NO through an inner-sphere electron-transfer reaction to produce the final product $[Co(P)(NO^-)]$. At pH < 3, the intermediate $[Co(P)(NO)(H_2O)]$ reacts with a second NO molecule to produce the final product. This subsequent reaction must be faster than the primary coordination of NO (as discussed above), and we believe that it is faster than the decomposition of the $[Co(P)(NO)(H_2O)]$ intermediate and drives the reaction toward reductive nitrosylation.

The role of NO_2^- is quite controversial, since it allows an alternative path for the reaction to occur, but under certain conditions (viz. a low pH or large excess of nitrite at pH > 3) it diminishes the yield of the final product. In the case of the $[Co(TPPS)(H_2O)_2]$ complex, for the reaction at low pH where the reaction with NO_2^- is prevented, the final product is generated faster, but in a lower yield probably due to the oxidizing effect of HNO_2. In contrast, for the $[Co(TMPyP)(H_2O)_2]$ complex the reaction with NO (low pH) is very slow, and the coordination of one NO_2^- molecule generates an intermediate which is more reactive toward NO, which allows us to conclude that NO_2^- catalysis occurs for this complex.

A final comment concerns the reaction of aquacobalamin (B_{12a}) with NO. In principle, it reacts only at low pH, where the protonation and labilization of the coordinated dimethylbenzimidazole group is favored.[3,4] At higher pH, the primary interaction between NO and B_{12a} would generate an intermediate of the type $[Co^{III}(L)NO]$, similar to the ones described in eqs 6 and 12. In the present report, we found in agreement with literature data that such intermediates are very unstable toward the dissociation of NO,[7] and reductive nitrosylation is observed only under conditions where a subsequent reaction with NO is possible (eqs 10, 14, and 15). In the case of B_{12a}, the availability of a second vacant coordination site at low pH would allow the possible coordination of a second NO molecule which can stabilize the intermediate(s) and allow reductive nitrosylation to proceed.

We are presently revisiting the reaction between B_{12a} and NO as a function of pH and the NO and NO_2^- concentrations. The reaction occurs only at low pH, as reported before.[3,4] In contrast, our preliminary results show that reductive nitrosylation is preceded by a fast reaction step that depends only on the NO_2^- concentration. In this way, the reactivity of B_{12a} has some similarity with that of the $[Co(TMPyP)(H_2O)_2]^{5+}$ complex. The intermediate is in principle a nitrite complex that is protonated at low pH and reacts further with NO. The detailed characteristics of these reaction steps are under investigation.

Acknowledgment. The authors gratefully acknowledge the financial support from the Deutsche Forschungsgemeinschaft through SFB 583 "Redox-active Metal Complexes" and the National Research Council of Argentina, CONICET.

Supporting Information Available: Figures: S1, titration of the $[Co(TPPS)(H_2O)_2]$ complex with NO; S2, determination of the NO_2^- formation; S3, UV−vis difference spectra of Figure 2; S4, plots of k_{obs} vs $[HNO_2]$ with and without NO for the $[Co(TPPS)(H_2O)_2]$ complex; S5, EPR spectrum of a $[Co(TPPS)(H_2O)_2]$ complex solution saturated with NO at pH 1.0; S6, plots of k_{obs} vs [NO] for the $[Co(TCPP)(H_2O)_2]$ complex; S7, plots of k_{obs} vs $[NO_2^-]$ for the $[Co(TCPP)(H_2O)_2]$ complex; S8, plots of k_{obs} vs [NO] for the $[Co(TMPyP)(H_2O)_2]$ complex; S9, plots of k_{obs} vs $[NO_2^-]$ for the $[Co(TMPyP)(H_2O)_2]$ complex. Table S1, detailed kinetic data for the $[Co(TPPS)(H_2O)_2]$ complex; Table S2, detailed kinetic data for the $[Co(TCPP)(H_2O)_2]$ complex; Table S3, detailed kinetic data for the $[Co(TMPyP)(H_2O)_2]$ complex. This material is available free of charge via the Internet at http://pubs.acs.org.

JA0549906